THE JOURNAL OF PHYSICAL CHEMISTRY B

Article

pubs.acs.org/JPCB

Molecular Dynamics Investigations of PRODAN in a DLPC Bilayer

William K. Nitschke,[†] Cíntia C. Vequi-Suplicy,[‡] Kaline Coutinho,[‡] and Hubert Stassen*,[†]

[†]Grupo de Química Teórica, Instituto de Química, UFRGS Av. Bento Gonçalves 9500, 91540-000 Porto Alegre, Brazil

[‡]Instituto de Física, Universidade de São Paulo, CP 66318, 05315-970 São Paulo, Brazil

ABSTRACT: Molecular dynamics computer simulations have been performed to identify preferred positions of the fluorescent probe PRODAN in a fully hydrated DLPC bilayer in the fluid phase. In addition to the intramolecular charge-transfer first vertical excited state, we considered different charge distributions for the electronic ground state of the PRODAN molecule by distinct atomic charge models corresponding to the probe molecule in vacuum as well as polarized in a weak and a strong dielectric solvent (cyclohexane and water). Independent on the charge distribution model of PRODAN, we observed a preferential orientation of this molecule in the bilayer with the dimethylamino group pointing toward the membrane's center and the carbonyl oxygen toward the membrane's interface. However, changing the charge distribution model of PRODAN, independent of its initial position in the equilibrated DLPC membrane, we observed different preferential positions. For the ground state representation without polarization and the in-cyclohexane polarization, the probe maintains its position close to the membrane's center. Considering the in-water polarization model, the probe approaches more of the polar headgroup region of the bilayer, with a strong structural correlation with the choline group, exposing its oxygen atom to water molecules. PRODAN's representation of the first vertical excited state with the in-water polarization also approaches the polar region of the membrane with the oxygen atom exposed to the bilayer's hydration shell. However, this model presents a stronger structural correlation with the phosphate groups than the ground state. Therefore, we conclude that the orientation of the PRODAN molecule inside the DLPC membrane is well-defined, but its position is very sensitive to the effect of the medium polarization included here by different models for the atomic charge distribution of the probe.

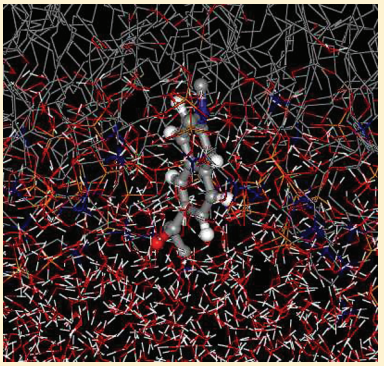

1. INTRODUCTION

6-Propionyl-2-(*N*,*N*-dimethylamino)naphthalene (PRODAN, see Figure 1) exhibits remarkable solvatochromic effects in absorption and, especially, emission spectra.[1] Experimentally observed fluorescence maxima are shifted by several thousands of wavenumbers going over from apolar to polar protic solvents.[1−3] PRODAN has been widely applied in experimental studies on solvation dynamics in different classes of solvents.[4] The high sensitivity toward environmental effects on the band positions of the emission spectra has been utilized to probe the local vicinity in biological systems such as proteins,[5] DNA,[6] and membranes.[7] Additionally, several experimental fluorescence studies on PRODAN coupled to micellar systems and vesicles have been published.[8]

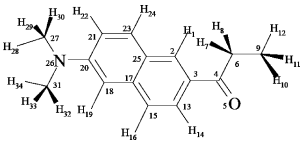

Figure 1. PRODAN molecule and atom numbering used in the present study.

In the present study, we are interested in the interaction of the PRODAN molecule with lipid bilayers. Temperature effects on the Stokes shift in fluorescence spectra of PRODAN in phospholipidic environments have been correlated with phase transitions and local polarities.[9] Experimental fluorescence spectra of PRODAN (and fluorophores with the same chromophore) in hydrated dilauroyl-phosphatidylcholine (DLPC) and dipalmitoyl-phosphatidylcholine (DPPC) bilayers exhibit two bands that have been interpreted to stem from the partitioning of the probe between the lipophilic and the polar regions of the bilayer.[10,11] The temperature dependence in these spectra is explained by changes in the membrane's fluidity affecting directly its hydration properties.[10] On the basis of these interpretations, a schematic representation has been proposed for the location of the fluorophores in the lipid bilayer with PRODAN's naphthalene unit close to the phospholipids' carbonyl groups and PRODAN's amino group directed toward the hydration shell.[12] A slightly different model for the interaction of PRODAN with the phospholipid bilayer has been developed from pressure dependent fluorescence studies.[13] In this model, the PRODAN molecule is located within the membrane's hydration shell but is enabled to flip the amino and naphthalene units into the more lipophilic environment. Fluorescence studies varying the phospholipid concentration have also been interpreted assuming the PRODAN molecule arranged in both the polar and the less polar regions of the bilayer.[14] The amphiphilic behavior of the

Received: September 5, 2011
Revised: February 1, 2012
Published: February 13, 2012

PRODAN molecule has been corroborated by infrared[15] and Raman[16] studies.

On the basis of pressure dependent experimental fluorescence studies on giant multilamelar vesicles containing lipids with phosphatidylcholine headgroups, the PRODAN molecule has been localized not only close to the glycerol backbone but also in the hydrophilic part of the membrane.[17] Correlating the observed fluorescence behavior with changes in the dielectric profile of the lipid bilayer, the probe molecule is believed to be located close to glycerol units in the gel phase, close to the phosphate groups in the liquid-crystalline phase, and near the head groups in the interdigitated gel phase.[18] Recently, Marsh applied reaction field models to spin-label electron paramagnetic resonance spectra in DPPC membranes and correlated PRODAN's Stokes shift quantitatively with the insertion depth of the probe molecule into the membrane. In DPPC bilayer, this correlation predicts a significant change in PRODAN's Stokes shift in the region of carbon 8 in the lipid's chain.[19]

In addition to changes in the partitioning of the PRODAN molecule in the amphiphilic environments, the dual fluorescence behavior of the PRODAN molecules in heterogeneous systems such as reverse micelles has been interpreted to stem from two distinct emitting states. On the basis of experimental observations, it is assumed that a local excited (LE) state is responsible for the emission in less polar media, whereas an intramolecular charge transfer (ICT) state determines the spectra in polar environments.[20] Fluorescence studies on PRODAN in reverse micelles present dual fluorescence believed to stem from both, the LE and the ICT states.[21]

In this article, we present results from molecular dynamics (MD) computer simulations for systems containing the PRODAN molecule interacting with a fully hydrated DLPC bilayer. The main purpose of the present study is the elucidation of structural properties for the PRODAN molecule within the phospholipidic environment to furnish detailed information about the location of the probe molecule. The computer simulation of models for biological membranes[22] nowadays represents a standard approach for the microscopic study of these complex systems[23] and has already been applied to study the interaction of membrane probes in bilayers.[24,25] The MD simulation technique has been very important in revealing perturbative effects of probe molecules on membrane properties such as area per lipid, bilayer thickness, order parameter, electrostatic potential along the membrane, lateral diffusion, and rotational dynamics of the lipid molecules.[25,26] In the case of PRODAN, this methodology has already been adopted to characterize the probe molecule's behavior in a dioleoyl-phosphatidylcholine (DOPC) bilayer model.[27,28]

2. FORCE FIELD

The molecular structure of PRODAN is illustrated in Figure 1. Its absorption and emission spectra have been the subject of several theoretical investigations. Earlier quantum mechanical (QM) studies revealed a planar ground and excited state with the possibility of twisting the dimethylamino and the carbonyl group upon ICT.[29,30] However, recent and more sophisticated calculations illustrate that the first excited state of the PRODAN molecule is planar[31,32] and other excited states are unlikely to be populated due to the very low oscillator strength for the ground to excited state transition.[31] Furthermore, constraining the dialkylamino group[3,33] and the carbonyl group[34] in PRODAN derivatives to the planar geometry presents fluorescence behavior very similar to that of PRODAN. Therefore, we assume in our parametrization procedures that both the ground and the excited state of the PRODAN molecule are planar. Furthermore, it has been shown that changes in the molecular geometry upon excitation are rather small,[31] which motivated us to use the same molecular geometries for the ground and the excited state as a starting point for the force field parametrizations. Although not further considered in the present work, it is worthwhile to mention that twisting the dimethylamino group in the excited state does not interfere in the penetration depth of the molecule.[28]

Quantum mechanical calculations on PRODAN's ground state have been undertaken at the B3LYP/6-31G(d) level with the Gaussian03 package[35] starting the geometry optimization from crystal structure data.[29] The obtained bond lengths, angles, and dihedrals are in good agreement with published data.[31] Afterward, atomic point charges were computed from single point calculations applying the CHELPG formalism[36] at the MP2/aug-cc-pVDZ level. The obtained point charges are summarized as charge set 1 (CS1) in the first column of Table 1.

Table 1. Atomic Charge (in units of *e*) for the PRODAN Molecule Used in the Simulations[a]

atom	CS1	CS2	CS3	CS4
H1	0.131	0.151	0.165	0.171
C2	−0.324	−0.272	−0.221	−0.194
C3	0.014	−0.065	−0.157	−0.154
C4	0.364	0.456	0.601	0.568
O5	−0.444	−0.537	−0.761	−0.927
$CH_2$6	0.123	0.118	0.141	0.179
$CH_3$9	−0.062	−0.052	−0.040	−0.031
C13	−0.059	−0.009	0.019	0.051
H14	0.083	0.109	0.097	0.112
C15	−0.198	−0.322	−0.356	−0.406
H16	0.109	0.139	0.163	0.163
C17	0.133	0.294	0.322	0.364
C18	−0.376	−0.539	−0.608	−0.599
H19	0.174	0.220	0.245	0.239
C20	0.274	0.395	0.430	0.447
C21	−0.146	−0.269	−0.274	−0.298
H22	0.127	0.153	0.171	0.176
C23	−0.272	−0.204	−0.209	−0.178
H24	0.129	0.146	0.168	0.170
C25	0.235	0.127	0.105	0.087
N26	−0.275	−0.284	−0.291	−0.246
$CH_3$27	0.125	0.122	0.144	0.152
$CH_3$31	0.135	0.123	0.146	0.154
μ_{QM}	5.8	6.1	10.2	14.7
μ_{MD}	5.5	5.7	8.9	13.2

[a]The atom numbering corresponds to that in Figure 1 with unified CH_2 and CH_3 groups. CS1 corresponds to the ground state in vacuum, CS2 to the ground state polarized in cyclohexane, CS3 to the ground state polarized in water, and CS4 to the first vertical excited state polarized in water. Also listed are molecular dipole moments (in D) from the QM (μ_{QM}) calculations and the point charge models (μ_{MD}).

To account for solvent effects on PRODAN's ground state, two additional charge sets have been considered by polarizing the obtained geometry in the solvents cyclohexane and water using the iterative sequential QM/MM procedure described elsewhere.[37] We preferred this approach when compared to the

dx.doi.org/10.1021/jp2085582 | J. Phys. Chem. B 2012, 116, 2713−2721

more common continuum models by considering explicitely the formation of hydrogen bonds between PRODAN's carbonyl oxygen and water hydrogens.[31,32] Cyclohexane has been chosen to mimic the weak dielectric environment within the lipophilic region of the bilayer, whereas water represents the environment in the polar headgroup region of the membrane. The atomic charges were computed at the level of theory described above and are included in Table 1 as charge sets 2 (CS2) and 3 (CS3) corresponding to the polarization scheme in cyclohexane and water, respectively.

A fourth set of point charges (CS4) has been computed for the first vertical excited state of PRODAN in the planar geometry optimized at RCIS/6-31G(d). The obtained charge distribution for this excited state in the gas phase that might correspond to the experimentally proposed LE state is very similar to the CS3 and therefore has not been taken into consideration for our simulation studies. However, polarizing in water at the same quantum mechanics level/basis, the dipole moment for this excited state is significantly increased. The corresponding point charges define the CS4 charge set detailed in the last column of Table 1.

To establish a topology for the ground state of PRODAN, we submitted the molecule as shown in Figure 1 to the beta PRODRG server.[38] We have chosen the topology corresponding to the GROMOS9653a6 (G53a6) force field.[39] This particular force field considers explicitely PRODAN's aromatic hydrogen atoms but treats the methyl and methylene groups as united atoms. Combining the topology proposal with the charge models CS1, CS2, and CS3, we accepted the obtained force field for the three ground state descriptions of PRODAN after verifying carefully energy minimizations and MD simulations of the isolated models. The topology for the excited state of PRODAN was achieved by the same procedure submitting a zwitterionic model of PRODAN carrying a positive nitrogen and a negative oxygen to the beta PRODRG server. Combining the G53a6 topology with the CS4 charge set, we obtained the force field for the first vertical excited state of the PRODAN molecule. Comparing the topologies for the ground and the first vertical excited state, we observed only minor differences: the carbonyl oxygen (atom type O of the G53a6 force field) of the ground state is substituted by the OA atom type (representing hydroxyl, sugar, or ester oxygen) in the excited state. As a consequence, intramolecular potential parameters for bond stretching and angle deformations as well as the Lennard-Jones parameters involving the oxygen atom are different in the two topologies.

The DLPC molecules have been described by the Berger force field for lipid molecules.[40] This particular force field is a united atom model derived from the Optimized Potential for Liquid State Simulations (OPLS) force field[41] with modified charges.[42] Recently, the Berger force field has been adapted to match intermolecular interactions with molecules described by the G53a6.[43] Water molecules have been described by the simple point charge model (SPC)[44] and cyclohexane by the G53a6 force field.

To our knowledge, there are three publications describing MD simulations on systems containing the PRODAN molecule. Marini et al. examined hydrogen bonding of PRODAN's ground and excited state in water and methanol.[32] The authors described the PRODAN molecule by the general AMBER force field[45] with Merz−Kollman charges[46] and the water molecules by the TIP3P model.[47] The other publications describe MD simulations of the ground and excited state of PRODAN in a DOPC bilayer.[27,28] In ref 27, the authors applied the CHARMM27 force field[48] to the DOPC molecules, the TIP3P model to the water molecules, and no further detailed particular parametrizations combined with Mulliken charges[49] to the PRODAN molecule. In ref 28, the united atom GROMOS force field[50] combined with Merz−Kollman charges was employed to planar and twisted configurations of PRODAN, the Berger force field to DOPC, and the SPC model to the water molecules. Thus, our MD simulations are complementary not only with respect to the choice of the phospholipids but also with respect to the selected force field. In the results section of the present work, we compare our findings with observations from the other MD investigations.[27,28,32]

3. COMPUTATIONAL DETAILS OF THE SIMULATIONS

All MD simulations have been performed with the GROMACS package, version 4.0.5.[51] Simulation boxes were built using version 3.3.2 of the GROMACS package.[52] All the simulations detailed below were carried out at constant pressure (1 bar, Parrinello-Rahman barostat[53]) and temperature (physiological temperature of 310 K, Nosé−Hoover thermostat[54]). In simulations with bilayers, we utilized the semiisotropical barostat maintaining independently the pressure within the bilayer's plane and perpendicular to it. If necessary, short steepest descent energy minimizations have been performed before initializing the MD simulations. The equations of motions have been integrated using a time-step of 2×10^{-15} s. The simulations have been extended to 10 ns in the case of diluted solutions of PRODAN in water and cyclohexane and to 40 ns in systems containing bilayers. Initial particle velocities have been chosen from a Maxwell−Boltzmann distribution corresponding to the desired temperature of the simulations.

Periodic boundary conditions have been employed in the simulations. Spherical cutoff radii of 1.5 nm have been defined for the neighbor list with an update frequency of 10 integration time-steps, the van der Waals interactions (correcting only energy and pressure), and the Coulomb interactions that were long-range corrected by a fourth order particle mesh Ewald approach.[55] We kept all the bond lengths constrained to the equilibrium distances defined by the force field employing the SETTLE algorithm[56] to water molecules and the LINCS algorithm[57] to the other molecule types.

The water box containing 216 molecules coming with the GROMACS package was used for hydration. A cube with 1000 cyclohexane molecules was created from a single molecule employing the genconf program of the GROMACS package. Both solvent boxes were equilibrated to match the desired temperature and pressure.

A PRODAN molecule with coordinates from the QM calculations was centered in a cubic box with dimensions of 6 nm and adapted to the G53a6 force field by energy minimization. Using the genbox program of the GROMACS package, the PRODAN molecule was solvated with the solvent boxes to create the diluted solutions in water (6991 water molecules) and cyclohexane (1201 solvent molecules).

To construct the hydrated DLPC bilayer, we started from an equilibrated hydrated palmitoyl-oleoyl-phosphatidylethanolamine (POPE) bilayer downloaded from Peter Tieleman's homepage[58] containing 340 lipid molecules. The coordinate and topology files were edited transforming the ethanolamine headgroup into choline and the particularities for the oleoylic double bond into definitions for the laureoylic single bond.

dx.doi.org/10.1021/jp2085582 | J. Phys. Chem. B 2012, 116, 2713−2721

Unnecessary CH_2 sites were cut out. After a short simulation, we increased the z axis (the normal to the plane containing the bilayer) and centered the entire system in the new box using GROMACS's editconf program. Free space was filled by additional water molecules by GROMACS's genbox routine. Several water molecules artificially introduced into the lipophilic environment were removed. This system, containing 340 DLPC and 17529 water molecules, was simulated for 40 ns.

Bilayer systems containing PRODAN were built starting from empty triclinic boxes with the same box dimensions of the equilibrated hydrated DLPC system. Two PRODAN molecules were centered at $x/4$, $y/2$, $z/2$ and $3x/4$, $y/2$, $z/2$, respectively, with the principal axis oriented along the z axis. Using the genbox program from the GROMACS package, the two PRODAN molecules were solvated with the equilibrated and hydrated DLPC bilayer. During this solvation process, we lost 28 DLPC molecules. Combining one of the PRODAN molecules with the topology for the CS1 charge set and another with the CS4 charge set, a simulation box containing 312 DLPC molecules, 17529 water molecules, and the two PRODANs was created. By combining the two PRODAN molecules with the topologies for the CS2 and CS3 charge sets, another system with the same initial conditions for the environment of the probe molecules has been defined. During the simulations, we verified that the intermolecular distance between the PRODAN molecules did not approach the established cutoff distances.

Structural properties for the simulated systems have been elucidated using programs from the GROMACS package: g_density for density profiles of the membrane, g_energy for monitoring the simulations (energies, sizes, interaction terms, etc.), g_rdf for radial pair distribution functions, g_mindist for minimum distances, g_angle for controlling angles and dihedrals within the PRODAN molecule, and g_dist for distances with respect to the center of the membrane.

4. RESULTS AND DISCUSSION

As mentioned before, we assumed PRODAN's ground and excited states as planar within the parametrization procedures. In MD simulations, thermal motion affects molecular geometries by angular and torsional deformations (note that the bond lengths have been constrained in the simulations). Thus, before starting a more detailed analysis of the simulated systems, we investigated the influence of thermal fluctuations on the molecular geometries. Out of plane motions of the naphthalene unit have been observed visually as related in MD simulations on the isolated molecules.[59] More important are the torsional motions involving the bonds between the naphthalene unit and the substitutions at C3 and C20 as well as the C4−O5 (see Figure 1). We have sampled the distributions of the corresponding improper dihedrals producing a Gaussian centered at 0° with halfwidths of ±10° for the C4−O5 and of ±7° for the C3−C4 improper dihedrals in the simulations of the CS1 and CS4 in the DLPC bilayer. In the case of the amino group, we analyzed the C20−N26 improper dihedral and the C18−C20−N26-C29 dihedral. We also observed averages indicating planarity in the CS1 and CS4 geometries. However, as shown in the distributions for the C20−N26 dihedral in Figure 2, we found maxima indicating two populated states with the methyl groups slightly above and below the planes of the naphthalene units. From these distributions of dihedral angles, we conclude that the planar structure of the PRODAN molecule is maintained on average

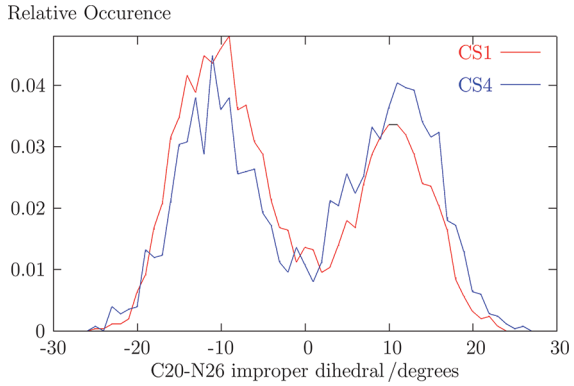

Figure 2. Distribution of improper dihedrals between C20 and N26 (see Figure 1) for the CS1 and CS4 charge sets of PRODAN in the DLPC bilayer.

and that thermal motion is responsible for weak distortions in this planarity. Our deviations from the planar geometry are smaller than observed in other simulation studies.[27,59]

The simulations of PRODAN in cyclohexane verified that structural correlation of the probe molecule with the solvent is weak. The CS1 and CS4 charge sets produce essentially identical RDFs (not shown) with the solvent's atoms, which is not surprising for very similar molecular geometries interacting with a solvent only by van der Waals interactions.

In aqueous PRODAN solutions, point charge interactions between the solute and the water molecules are important. The CS1 and CS4 charge sets involve quite different charge distributions (see Table 1) and one might expect distinct structural features in the RDFs. However, with the exception of PRODAN's carbonyl group, the site−site RDFs between PRODAN and the water molecules (not shown) are very similar for the two charge sets exhibiting only very weak correlations.

PRODAN's carbonyl oxygen represents a hydrogen bond acceptor. The corresponding RDFs (not shown) reveal some hydrogen bonding patterns involving on average 1.7 water protons in the CS1 and 3.4 water hydrogens in the CS4 solutions. These results are in good agreement with previous simulation studies on the excited state of PRODAN in water.[32]

4.1. PRODAN's Dipole Moment. The molecular dipole moment of the of the PRODAN molecule represents another important property with experimental relevance. We included PRODAN's dipole moments from the QM calculations and also averaged from the MD simulations in the bilayer systems in Table 1 for the different charge sets.

Our gas phase value of 5.8 D obtained with the QM treatment (MP2/aug-cc-pVDZ) is in very good agreement with theoretical estimates of 6.0 D obtained with DFT by other authors[32,60] and the experimental result of 5.2 D measured in benzene solution.[61] Solvent effects on PRODAN's ground state have been taken into account by the density functional theory (B3LYP/6-311+G(d,p)) with the polarizable continuum model (PCM)[62] producing dipole moments of 6.1 D in vacuum, 7.7 D in cyclohexane, and 9.4 D in water.[31] Our QM/MM approach furnishes a smaller dipole moment in cyclohexane (6.1 D), but a larger value (10.2 D) in water. The difference between the two dipole moments for the water environment is due to an inappropriate description of the continuum model for this hydrogen bonding solvent. If two additional water molecules are placed close to PRODAN's oxygen, the dipole moment

from the dielectric continuum has been shown to increase to 13.2 D for the PRODAN + $2H_2O$ complex.[31] Surprisingly, the DFT-PCM approach produces an increase in PRODAN's dipole moment of 1.6 D upon solvation in cyclohexane, whereas our QM/MM approach furnishes a difference of only 0.3 D between the cyclohexane solution and the vacuum. Therefore, we performed an additional QM calculation on PRODAN's ground state using the conventional PCM.[63] This calculation furnishes a dipole moment of 6.2 D in very good agreement with our QM/MM result. Comparing the dipole moments for the different solvents, it becomes evident that polarization effects are important, especially in polar solvents, for an adequate atomic charge model of PRODAN.

The dipole moment for the first vertical excited state of the PRODAN molecule is also discussed in the literature.[31,32,60] Our numerical values are 11.5 D in vacuum obtained with RCIS/6-31G(d) and 14.7 D polarized in water with our QM/MM approach. The in-vacuum value is within the range of previously calculated data and the experimental result of 10.2 D measured in cyclohexane.[61] Our in-water value is in good agreement with a previously calculated value of 13.8 D obtained from TD-DFT.[32]

The dipole moments averaged from the MD simulations are smaller than the values obtained by QM methods (Table 1). The reason for these differences is mainly due to the united atom description for the methyl and methylene groups in our PRODAN model. Note that these groups are far from the charge center of the molecule and small changes in both charges and distances are expected to produce effects in the overall dipole moment.

4.2. PRODAN in a DLPC Bilayer. Before discussing our results for the fluorophore within the bilayer, we present some properties for the hydrated DLPC bilayer, which is in the fluid phase at the simulated temperature of 310 K.[64] Using the semiisotropic barostat, we are able to compute the area for a single DLPC molecule in the bilayer from the product of the boxsizes in x and y directions divided by the number of DLPC molecules in a leaflet yielding a value of 60.6 ± 0.4 Å^2 for our membrane. The insertion of the PRODAN molecule does not change this value. There are several experimental estimates of the area per phospholipid for a DLPC bilayer with values between 57.2 and 71 Å^2 for the fluid phase.[65,66] MD simulations on DLPC bilayers also furnished the area per phospholipids. We cite numerical values[67] of 62.9, 65.0, and 56.1 Å^2 obtained from DLPC parametrizations based on the GROMOS force field 43a1-S3,[67] the force field used in our study,[40] and the G53a6 with modified charges from Chiu et al.,[42] respectively, with the water molecules described by the extended SPC model (SPC/E).[68] At slightly higher temperature (323 K), the force field used by us furnished a value of 66 Å^2.[69] From a distinct parametrization of the G53a6 for phospholipids,[70] 63.2 Å^2 has been obtained.[71] Thus, our calculated value for the area per DLPC molecule of 60.6 Å^2 is within the range of these previously published data.

In Figure 3, the electron density profile of the simulated DLPC bilayer is presented. The distance between the two maxima is utilized to define the bilayer thickness as 2.9 ± 0.1 nm, which is in good agreement with experiment (3.08 nm[66]). The three simulations performed by Chiu et al.[67] produced 2.85, 2.78, and 3.10 nm with the GROMOS 43a1-S3, the force field used in our study, and the G53a6, respectively. The reparameterized G53a6 furnished 2.85 nm for the DLPC bilayer's thickness.[71] In summary, the comparison with the literature values demonstrates that our DLPC bilayer model describes correctly the height of the membrane.

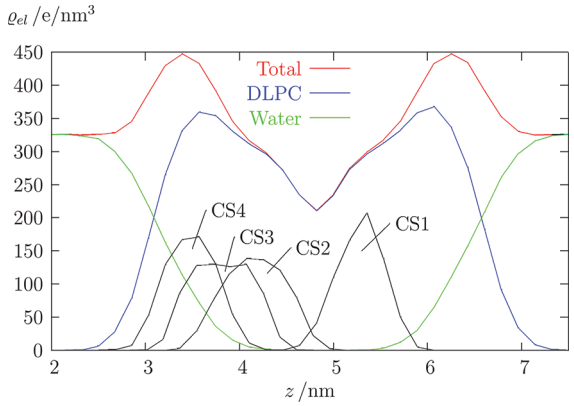

Figure 3. Electron density profile of the DLPC bilayer and the contributions stemming from the DLPC, water, and PRODAN molecules. The electron density profiles for the four charge sets of the PRODAN molecule have been multiplied by 100.

The insertion of PRODAN into a lipid bilayer can be observed by MD simulations.[27,28] However, we started our simulations with the four charge sets of PRODAN centered in the DLPC membrane with its principal axis oriented in parallel to the normal of the bilayer's surface. We monitored the localization of PRODAN's nitrogen and oxygen atoms during the simulations. In Figure 4, we present the time evolution for

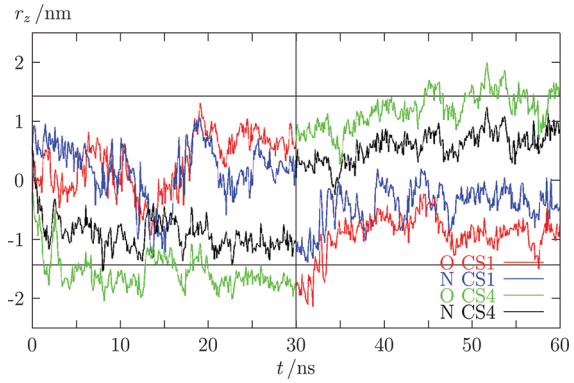

Figure 4. Time evolutions for distances between the center of the bilayer (the minimum in the electron density profile from Figure 3) and the z coordinates of the oxygen and nitrogen atoms for the CS1 and CS4 charge sets of PRODAN. At t = 30 ns, the charge sets have been inverted. Vertical lines indicate the maxima of the electron density profile from Figure 3.

the z coordinates relative to the bilayer's center of these atoms within the membrane for the charge sets CS1 and CS4. Note that we inverted the charge sets CS1 → CS4 and CS4 → CS1 at 30 ns in order to mimic the electronic excitation and deactivation of the probe molecules. In any case, we observe that the charge sets achieve an equilibrium localization within the bilayer after 20 ns. If we compare the positions of the nitrogen and oxygen atoms of both charge sets, we find the nitrogen atoms closer to the bilayer's center. The trajectories also demonstrate that our excited state representation CS4 approaches the hydration shell, whereas CS1 remains closer to the center of the membrane. Along the trajectories, the CS4 charge set exposes its oxygen toward the polar headgroup region. In the case of the CS1 charge set, we observe especially

dx.doi.org/10.1021/jp2085582 | J. Phys. Chem. B 2012, 116, 2713–2721

during the first 20 ns changes in the orientation of the PRODAN molecule relative to the bilayer's interface several times crossing between the lower and upper layers. After inversion of the two charge sets at 30 ns, we obtained trajectories confirming the mentioned features. Unfortunately, the illustrated trajectories do not permit the definition of a concrete time scale for the motion of CS1 toward the internal part of the membrane and CS4 in direction to the hydration layer.

To characterize in more detail the positions of the four charges sets for the PRODAN molecule, we included their electron density profiles in Figure 3 obtained as averages over the last 5 ns of the simulations. From this figure, it becomes evident that PRODAN's charge distribution is very important for the localization of the probe molecule. We observe a gradual shift toward the hydrated polar region of the bilayer by increasing the fluorophore's dipole moment. For the charge distribution corresponding to PRODAN's ground state in vacuum (CS1), the electron density profile demonstrates that the environment is lipophilic. However, the excited state charge distribution in the CS4 set approached the hydration shell of the bilayer. The electron density profiles of the four charge sets are approximately Gaussian as observed in simulations of the PRODAN molecule in a DOPC bilayer.[27] The maximum positions relative to the minimum in the total electron density profile, i.e., relative to the center of the bilayer, are 0.54, 0.64, 0.99, and 1.32 nm for the CS1, CS2, CS3, and CS4 charge sets with a statistical error of ±0.03 nm. Barucha-Kraszewska et al.[27] determined these distances in a hydrated DOPC bilayer between 1.2 and 1.7 nm for the center of PRODAN's ground state and between 1.3 and 1.8 nm for the center of the excited state. The DOPC bilayer is composed by phospholipids containing 18 carbons in the aliphatic chains, whereas the DLPC molecules contain only twelve aliphatic carbon atoms. Thus, considering the difference of six carbons in the investigated lipid molecules, we may conclude that the insertion depth of the probe molecules in both bilayers is very similar. In contrast, Cwiklik et al.[28] observed a deeper insertion of the PRODAN molecule into the DOPC bilayer without any changes in the penetration depth for the ground and excited states.

More details for the probe's localization within the bilayer are discussed in the following using RDFs for distances between the PRODAN molecule and the lipid bilayer. We have chosen the methyl substitutions in the amino group as well as the carbonyl oxygen of the PRODAN molecule as references. These atoms may be considered to represent the edges of the chromophore. The bilayer has been sectioned into seven particular regions: water, DLPC's choline group, the phosphate group, the glycerol unit, the carbonyl groups, the first five carbons in the aliphatic chain, and the last six carbons in the DLPC's tails.

The RDFs for the amino methyls and these seven groups are illustrated in Figure 5 considering the four charge sets. Shortest distances involving these methyl groups appear at 0.3 nm for all the charge sets. To be more specific, nearest neighbor configurations of these methyl groups are observed with DLPC's carbonyl groups independent of PRODAN's charge distributions. However, these configurations produce only very small amplitudes in the RDFs for the CS1 and CS2 charge sets. The point charges on the amino methyl groups are positive (see Table 1) and electrostatic interactions with the negative

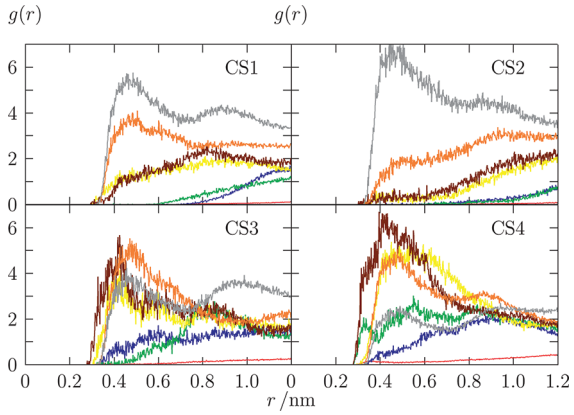

Figure 5. RDFs of PRODAN's amino methyl groups with parts of the DLPC molecules in the bilayer for charge sets CS1 (upper left), CS2 (upper right), CS3 (lower left), and CS4 (lower right). The colors indicate RDFs with the water oxygens (red), DLPC's choline group (blue), the phosphate group (green), the glycerol unit (yellow), DLPC's carbonyl groups (brown), DLPC's first five aliphatic methylenes (orange), and the last six carbons in DLPC's chain (gray).

charged carbonyl oxygens of the DLPC molecules might be responsible for these nearest neighbor configurations.

As shown in Table 1, PRODAN's dipole moment increases in the investigated series of charge sets from CS1 to CS4. In Figure 3, we observed that more polar charge sets are shifted toward the polar headgroup region of the bilayer. This tendency is also observed in the RDFs from Figure 5. The less polar charge distributions CS1 and CS2 present the largest amplitudes for correlations of the amino methyl groups with the aliphatic tail groups of the DLPC molecules. For the charge sets CS3 and CS4, DLPC's more internal aliphatic methylene groups, DLPC's carbonyl groups, and the glycerol units become very important. For PRODAN's excited state (CS4), we observe also significant short-range correlations with the lipid's phosphate group. The RDFs for distances to the choline groups and water molecules are less important. In summary, PRODAN's amino group is buried within the lipophilic environment of the membrane for the charge sets CS1 and CS2 approximating the membrane's glycerol units in the cases of the more polar charge representations CS3 and, especially, CS4.

The RDFs for the CS1 charge set indicate a more polar environment in the vicinity of the amino group than for the CS2 charge distribution although the dipole for CS2 is slightly larger than for CS1. We attempt to explain this observation by local perturbations of the bilayer due to the presence of the CS1 charge set as argued below.

In Figure 6, we present the RDFs for PRODAN's carbonyl oxygen with the seven groups of the DLPC molecules. We find correlations between PRODAN's oxygen and parts of the DLPC molecules starting at 0.3 nm. In addition, we observe increasing hydrogen bonding by the water protons in the series of charge sets CS2, CS3, and CS4 in Figure 6 at distances also detected in aqueous solutions. In the case of charge set CS1, these correlations are absent. Integrating the first peak in the RDFs for the water hydrogens, we find coordination numbers of 0.8 for CS2 and 2.3 for CS3. In the case of the excited state representation CS4, this integral yields 3.4 water protons close to the oxygen as found in the water solutions. Comparing the peak height of this particular RDF in the bilayer (≃8) and the water solution (≃5), we deduce that this peak is sharpened in

dx.doi.org/10.1021/jp2085582 | J. Phys. Chem. B 2012, 116, 2713–2721

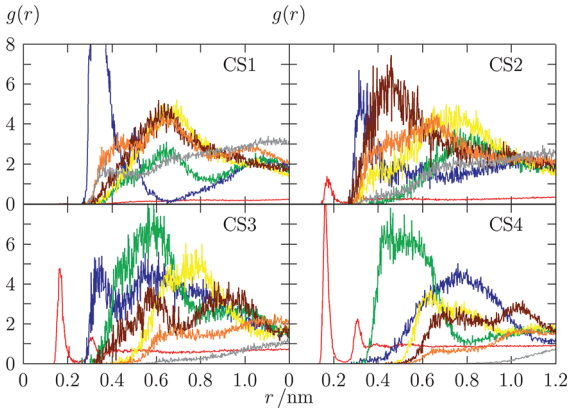

Figure 6. RDFs of PRODAN's carbonyl oxygen with parts of the DLPC molecules in the bilayer for charge sets CS1 (upper left), CS2 (upper right), CS3 (lower left), and CS4 (lower right). The colors indicate RDFs with the water hydrogens (red), DLPC's choline group (blue), the phosphate group (green), the glycerol unit (yellow), DLPC's carbonyl groups (brown), DLPC's first five aliphatic methylenes (orange), and the last six carbons in DLPC's chain (gray). The RDF involving the choline group and the charge set CS1 possesses a maximum amplitude of 13.

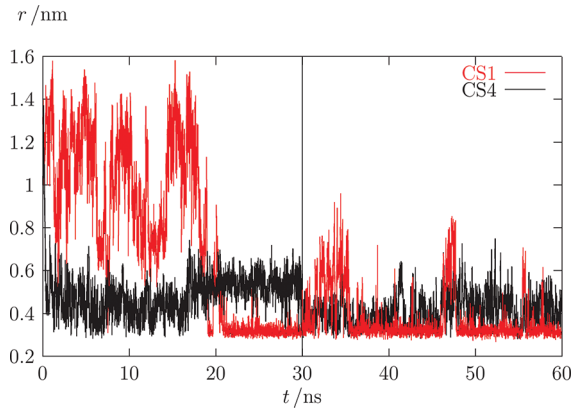

Figure 7. Time evolution of shortest distances between PRODAN's oxygen atom (CS1 and CS4 charge sets) and any atom belonging to the choline groups in the bilayer. Pieces of the trajectories exhibiting small oscillations of the red curve around 0.32 nm indicate complexation of PRODAN's oxygen by a single choline group. The charge sets have been inverted at t = 30 ns.

the bilayer system probably due to a higher ordering of the water molecules in the hydrated polar region of the membrane, already revealed experimentally.[72]

The RDFs for CS4 in Figure 6 demonstrate that PRODAN's carbonyl group is close to DLPC's phosphate groups possibly sharing the hydration shell. The other parts of the DLPC molecule appear at larger distances in the expected sequence: glycerol units, DLPC's carbonyl groups, and the aliphatic tails. Going over to the less polar charge sets, we observe that the DLPC's carbonyl group, the glycerol units, and the aliphatic tails approximate PRODAN's oxygen. In the case of the less polar CS1, all of these RDFs exhibit a strong increase in amplitude at similar distances between 0.3 and 0.4. nm.

The RDFs of PRODAN's carbonyl oxygen and DLPC's choline group in Figure 6 presents distinct features. For the excited state CS4, we do not observe short-range correlations in this RDF although PRODAN's oxygen possesses a large negative charge (Table 1) permitting strong electrostatic interactions with the positively charged methyl groups in the choline unit. However, both CS4's oxygen and the choline group are hydrated and, as our data indicate, prefer separate hydration shells. The choline headgroup in the bilayer is highly flexible, which facilitates its turn away from PRODAN's oxygen. In the CS3 charge set, PRODAN's oxygen charge is reduced when compared with CS4 (Table 1) and, as discussed before, its hydration shell weakened. As a consequence, we detect short-range correlations with DLPC's choline group possibly sharing hydration shells. This tendency is still more pronounced in the case of charge set CS2.

For charge set CS1, the RDF of PRODAN's oxygen with DLPC's choline group exhibits a huge short-range peak with maximum amplitude of 13 and an integral indicating four atoms (the three methyl groups and the nitrogen) of one distinct choline group in the oxygen's neighborhood. From the discussion above, we know that CS1's oxygen is far from the hydration layer of the membrane. Thus, we conclude that one of the DLPC molecules flips the choline group into the more lipophilic part of the bilayer coordinating CS1's carbonyl oxygen. In Figure 7, we illustrate the time evolution of the shortest distance between PRODAN's oxygen and atoms of the bilayer's choline groups. The CS4 and the CS1 charge sets are emphasized. The trajectory for this distance involving CS4 presents fluctuations about an average of approximately 0.5 nm, which is characteristic for the peakless RDF in Figure 6. However, the CS1 charge set exhibits the shortest distances fluctuating with small amplitudes about an average of 0.32 nm beyond 20 ns. This feature indicates a strong interaction furnishing the large peak in the corresponding RDF of Figure 6 at this distance. We mention that the coordination of CS1's oxygen by a single choline group might be occasional. However, as shown in Figure 7, the coordination by the choline group is also observed along several pieces of the trajectories with the charge sets inverted at 30 ns. Thus, we conclude that the combination of our force fields for the charge set CS1 and the DLPC molecules permits this kind of complexation.

We note that there are no experimental evidence for the strong coordination of PRODAN's carbonyl oxygen by the choline group. Vibrational spectroscopy of PRODAN's C−O double bond should be a reliable source for revealing such a strong interaction. However, the systematic FT-IR studies of Chong et al.[15] do not furnish any indication for a special interaction at PRODAN's carbonyl oxygen in lipid bilayers. If we consider the charge set CS2, Figure 6 demonstrates that an increase in PRODAN's dipole moment of only 0.2 D (see Table 1) weakens significantly the interaction with the choline group. Therefore, small polarization effects on the PRODAN molecule might be important for the realistic description of the probe molecule in a bilayer.

5. CONCLUSIONS

In the present article, we revealed detailed information about the localization of the PRODAN molecules in a fully hydrated DLPC lipid bilayer in the fluid phase using MD simulations. Special attention has been devoted to PRODAN's charge distribution by considering four different charge sets of the fluorophore. We observed that PRODAN's ground state described by the vacuum charge distribution CS1 is buried within the lipophilic part of the bilayer. The polarization effect on this charge distribution (CS2 polarized in cyclohexane and CS3 polarized in water) approaches the probe molecule to the

dx.doi.org/10.1021/jp2085582 | J. Phys. Chem. B 2012, 116, 2713−2721

more polar headgroup region of the membrane. The excited state is localized in the polar region part of the bilayer.

Independent on its charge distribution, we observed an orientation of the PRODAN molecule with the dimethylamino group pointing toward the membrane's center and the carbonyl oxygen toward the membrane's interface. In the case of the excited state, hydrogen bonding with the water molecules in the membrane's hydration layer has been revealed. We find nearly three water molecules bonded to the excited PRODAN in water solution and in the bilayer. The difference between both environments is the stronger correlation with water molecules in the hydration shell of the bilayer. From the electron density profiles, we found that smaller dipole moments of the PRODAN molecule increase the insertion depth of the probe molecule. Thus, polarization effects are important in detailed studies of probe molecules inserted in lipid bilayers.

Comparing with simulations on diluted solutions of PRODAN in water and cyclohexane, we found that the shortest distances for nearest neighbor configurations in these solutions are maintained in the bilayer system. Hydrogen bonding in the aqueous solution is observed only for the hydration shell at PRODAN's carbonyl oxygen. The observed hydrogen bonding patterns are significantly weaker in solutions of the ground state representation when compared to PRODAN's excited state. However, in the DLPC bilayer, PRODAN's ground and excited states are stronger coupled to the environment than in diluted cyclohexane and water solutions as indicated by the amplitudes in the RDFs from Figures 5 and 6. Details in these patterns depend on the polarization of the probe molecule.

AUTHOR INFORMATION

Corresponding Author

*E-mail: gullit@iq.ufrgs.br.

Notes

The authors declare no competing financial interest.

ACKNOWLEDGMENTS

K.C. and H.S. acknowledge funding from CNPq, nBioNet, and INCT-FCx; W.K.N. acknowledges a grant from Brazilian agency CAPES and C.C.V.-S. a fellowship from FAPESP.

REFERENCES

(1) Weber, G.; Farric, J. F. *Biochemistry* **1979**, *18*, 3075.
(2) Lakowicz, J. R.; Balter, A. *Biophys. Chem.* **1982**, *16*, 117, 223. Catalan, J.; Perez, P.; Laynez, J.; Blanco, F. G. *J. Fluoresc.* **1991**, *4*, 215. Kucherak, O. A.; Didier, P.; Mely, Y.; Klymchenko, A. S. *J. Phys. Chem. Lett.* **2010**, *1*, 616.
(3) Lobo, B. C.; Abelt, C. J. *J. Phys. Chem. A* **2003**, *107*, 10938.
(4) Chapman, C. F.; Fee, R. S.; Maroncelli, M. *J. Phys. Chem.* **1990**, *94*, 4929. Chapman, C. F.; Maroncelli, M. *J. Phys. Chem.* **1991**, *95*, 9095. Betts, T. A.; Zagrobelny, H.; Bright, F. V. *J. Am. Chem. Soc.* **1992**, *114*, 8163. Karmakar, R.; Samanta, A. *J. Phys. Chem. A* **2002**, *106*, 6670. Ito, N.; Arzhantsev, S.; Maroncelli, M. *Chem. Phys. Lett.* **2004**, *396*, 83.
(5) Moreno, F.; Cortijo, M.; Gonzalez-Jimenez, J. *Photochem. Photobiol.* **1999**, *69*, 8. Kamal, J. K. A.; Zhao, L.; Zewail, A. H. *Proc. Natl. Acad. Sci. U.S.A.* **2004**, *101*, 13411. Bhattacharyya, M.; Ray, S.; Bhattacharya, S.; Chakrabarti, A. *J. Biol. Chem.* **2004**, *279*, 55080.
(6) Tainaka, K.; Tanaka, K.; Ikeda, S.; Nishiza, L.; Unzai, T.; Fujiwara, Y.; Saito, I.; Okamoto, A. *J. Am. Chem. Soc.* **2007**, *129*, 4776.
(7) Massey, J. B.; She, H. S.; Pownall, H. J. *Biochemistry* **1985**, *24*, 6973. Rottenberg, H. *Biochemistry* **1992**, *31*, 9473. Bondar, O. P.; Rowe, E. S. *Biophys. J.* **1999**, *76*, 956. Hutterer, R.; Hof, M. *J. Fluoresc.* **2001**, *11*, 227. Kusube, M.; Matsuki, H.; Kaneshina, S. *Colloids Surf., B* **2005**, *42*, 78. Wilson-Ashworth, H. A.; Bahm, Q.; Erickson, J.; Shinkle, A.; Vu, M. P.; Woodbury, D.; Bell, J. D. *Biophys. J.* **2006**, *91*, 4091.
(8) Wong, J. E.; Duchscherer, T. M.; Pietraru, G.; Cramb, D. T. *Langmuir* **1999**, *15*, 6181. Karukstis, K. K.; Zieleniuk, C. A.; Fox, M. J. *Langmuir* **2003**, *19*, 10054. Sykora, J.; Jurkiewicz, P.; Epand, R. M.; Kraayenhof, R.; Langner, M.; Hof, M. *Chem. Phys. Lipids* **2005**, *135*, 213. Sachl, R.; Stepanek, M.; Prochazka, K.; Humpolickova, J.; Hof, M. *Langmuir* **2008**, *24*, 288.
(9) Hutterer, R.; Schneider, F. W.; Sprinz, H.; Hof, M. *Biophys. Chem.* **1996**, *61*, 151. Hutterer, R.; Parusel, A. B. J.; Hof, M. *J. Fluoresc.* **1998**, *8*, 389. Krasnowska, E. K.; Bagatolli, L. A.; Gratton, E.; Parasassi, T. *Biochim. Biophys. Acta* **2001**, *1511*, 330. Kozyra, K. A.; Heldt, J. R.; Gondek, G.; Kwiek, P.; Heldt, J. *Z. Naturforsch., A: Phys. Sci.* **2004**, *59*, 809.
(10) Krasnowska, E. K.; Gratton, E.; Parasassi, T. *Biophys. J.* **1998**, *74*, 1984.
(11) de Vequi-Suplicy, C. C.; Benatti, C. R.; Lamy, M. T. *J. Fluoresc.* **2006**, *16*, 431.
(12) Parasassi, T.; Krasnowska, E. K.; Bagatolli, L.; Gratton, E. *J. Fluoresc.* **1998**, *8*, 365.
(13) Chong, P. L. G. *Biochemistry* **1988**, *27*, 399.
(14) Moyano, F.; Biasutti, M. A.; Silber, J. J.; Correa, N. M. *J. Phys. Chem. B* **2006**, *110*, 11838. Moyano, F.; Molina, P. G.; Silber, J. J.; Sereno, L.; Correa, N. M. *ChemPhysChem* **2010**, *11*, 236.
(15) Chong, P. L. G.; Capes, S.; Wong, P. T. T. *Biochemistry* **1989**, *28*, 8358.
(16) Krilov, D.; Balarin, M.; Kosović, M.; Brnjas-Kraljević, J. *Eur. Biophys. J.* **2008**, *37*, 1105.
(17) Goto, M.; Sawaguchi, H.; Tamai, N.; Matsuki, H.; Kaneshina, S. *Langmuir* **2010**, *26*, 13377.
(18) Goto, M.; Kusube, M.; Nishimoto, M.; Tamai, N.; Matsuki, H.; Kaneshina, S. *Ann. N. Y. Acad. Sci.* **2010**, *1189*, 68.
(19) Marsh, D. *Biophys. J.* **2009**, *96*, 2549.
(20) Rollinson, A. M.; Drickamer, H. G. *J. Chem. Phys.* **1980**, *73*, 5981.
(21) Novaira, M.; Biasutti, M. A.; Silver, J. J.; Correa, N. M. *J. Phys. Chem. B* **2007**, *111*, 748. Novaira, M.; Moyano, F.; Biasutti, M. A.; Silber, J. J.; Correa, N. M. *Langmuir* **2008**, *24*, 4637. Adhikary, R.; Barnes, C. A.; Petrich, J. W. *J. Phys. Chem. B* **2009**, *113*, 11999.
(22) Tieleman, D. P.; Marrink, S. J.; Berendsen, H. J. C. *Biochim. Biophys. Acta* **1997**, *1331*, 235.
(23) Gurtovenko, A. A.; Anwar, J.; Vattulainen, I. *Chem. Rev.* **2010**, *110*, 6077.
(24) Repáková, J.; Čapková, P.; Holopainen, J. M.; Vattulainen, I. *J. Phys. Chem. B* **2004**, *108*, 13438. Gullapalli, R. R.; Demirel, M. C.; Butler, P. J. *Phys. Chem. Chem. Phys.* **2008**, *10*, 3548. Song, K. C.; Livanec, P. W.; Klauda, J. B.; Kuczera, K.; Dunn, R. C.; Im, W. *J. Phys. Chem. B* **2011**, *115*, 6157.
(25) Loura, L. M. S.; Prates Ramalho, J. P. *Biophys. Rev.* **2009**, *1*, 141.
(26) Repáková, J.; Holopainen, J. M.; Karttunen, M.; Vattulainen, I. *J. Phys. Chem. B* **2006**, *110*, 15403.
(27) Barucha-Kraszewska, J.; Kraszewski, S.; Jurkiewicz, P.; Ramseyer, C.; Hof, M. *Biochim. Biophys. Acta* **2010**, *1798*, 1724.
(28) Cwiklik, L.; Aquino, A. J. A.; Vazdar, M.; Jurkiewicz, P.; Pittner, J.; Hof, M.; Lischka, H. *J. Phys. Chem. A.* **2011**, *115*, 11428.
(29) Ilich, P.; Prendergast, F. G. *J. Phys. Chem.* **1989**, *93*, 4441.
(30) Nowak, W.; Adamczak, P.; Balter, A.; Sygula, A. *J. Mol. Struct.* **1986**, *139*, 13. Parusel, A. B. J.; Schneider, F. W.; Köhler, G. *J. Mol. Struct.* **1997**, *398*−*399*, 341. Parusel, A. B. J.; Nowak, W.; Grimme, S.; Köhler, G. *J. Phys. Chem. A* **1998**, *102*, 7149. Parusel, A. B. J. *J. Chem. Soc., Faraday Trans.* **1998**, *94*, 2923.
(31) Mennucci, B.; Caricato, M.; Ingrosso, F.; Cappelli, C.; Cammi, R.; Tomasi, J.; Scalmani, G.; Frisch, M. J. *J. Phys. Chem. B* **2008**, *112*, 414.
(32) Marini, A.; Muñoz-Losa, A.; Biancardi, A.; Mennucci, B. *J. Phys. Chem. B* **2010**, *114*, 17128.
(33) Davis, B. N.; Abelt, C. J. *J. Phys. Chem. A* **2005**, *109*, 1295.

(34) Everett, R. K.; Nguyen, H. A. A.; Abelt, C. J. *J. Phys. Chem. A* **2010**, *114*, 4946.
(35) Frisch, M. J.; Trucks, G. W.; Schlegel, H. B.; Scuseria, G. E.; Robb, M. A.; Cheeseman, J. R.; Montgomery, J. A., Jr.; Vreven, T.; Kudin, K. N.; Burant, J. C.; Millam, J. M.; Iyengar, S. S.; Tomasi, J.; Barone, V.; Mennucci, B.; Cossi, M.; Scalmani, G.; Rega, N.; Petersson, G. A.; Nakatsuji, H.; Hada, M.; Ehara, M.; Toyota, K.; Fukuda, R.; Hasegawa, J.; Ishida, M.; Nakajima, T.; Honda, Y.; Kitao, O.; Nakai, H.; Klene, M.; Li, X.; Knox, J. E.; Hratchian, H. P.; Cross, J. B.; Bakken, V.; Adamo, C.; Jaramillo, J.; Gomperts, R.; Stratmann, R. E.; Yazyev, O.; Austin, A. J.; Cammi, R.; Pomelli, C.; Ochterski, J. W.; Ayala, P. Y.; Morokuma, K.; Voth, G. A.; Salvador, P.; Dannenberg, J. J.; Zakrzewski, V. G.; Dapprich, S.; Daniels, A. D.; Strain, M. C.; Farkas, O.; Malick, D. K.; Rabuck, A. D.; Raghavachari, K.; Foresman, J. B.; Ortiz, J. V.; Cui, Q.; Baboul, A. G.; Clifford, S.; Cioslowski, J.; Stefanov, B. B.; Liu, G.; Liashenko, A.; Piskorz, P.; Komaromi, I.; Martin, R. L.; Fox, D. J.; Keith, T.; Al-Laham, M. A.; Peng, C. Y.; Nanayakkara, A.; Challacombe, M.; Gill, P. M. W.; Johnson, B.; Chen, W.; Wong, M. W.; Gonzalez, C.; Pople, J. A. *Gaussian 03*, revision D.01; Gaussian, Inc.: Wallingford, CT, 2003.
(36) Breneman, C. M.; Wiberg, K. B. *J. Comput. Chem.* **1990**, *11*, 361.
(37) Georg, H. C.; Coutinho, K.; Canuto, S. *Chem. Phys. Lett.* **2006**, *429*, 119. Coutinho, K.; Rivelino, R.; Georg, H. C.; Canuto, S. In *Solvation Effects on Molecules and Biomolecules*; Canuto, S., Ed.; Computational Methods and Applications Series: Challenges and Advances in Computational Chemistry and Physics; Springer: New York, 2008; Vol. *6*, p 159. Fonseca, T. L.; Georg, H. C.; Coutinh, K.; Canuto, S. *J. Phys. Chem. A* **2009**, *113*, 5112.
(38) The GlycoBioChem PRODRG2 Server. http://davapc1.bioch.dundee.ac.uk/cgi-bin/prodrg_bet (accessed April 04, 2011). Schuettelkopf, A. W.; van Aalten, D. M. F. *Acta Crystallogr.* **2004**, *D60*, 1355.
(39) Oostenbrink, C.; Villa, A.; Mark, A. E.; van Gunsteren, W. F. *J. Comput. Chem.* **2004**, *25*, 1656. Oostenbrink, C.; Soares, T. A.; van der Vegt, N. F. A.; van Gunsteren, W. F. *Eur. Biophys. J.* **2005**, *34*, 273.
(40) Berger, O.; Edholm, O.; Jähnig, F. *Biophys. J.* **1997**, *72*, 2002.
(41) Jorgensen, W. L.; Tirado-Rives, J. *J. Am. Chem. Soc.* **1988**, *110*, 1657.
(42) Chiu, S. W.; Clark, M.; Balaji, V.; Subramaniam, S.; Scott, H. L.; Jakobsson, E. *Biophys. J.* **1995**, *69*, 1230.
(43) Siu, S. W. I.; Vácha, R.; Jungwirth, P.; Böckmann, R. A. *J. Chem. Phys.* **2008**, *128*, 125103 see http://www.bioinf.uni-sb.de/RB/ (accessed April 05, 2011).
(44) Berendsen, H. J. C.; Postma, J. P. M.; van Gunsteren, W. F.; Hermans, J. In *Intermolecular Forces*; Pullman, B., Ed.; Reidel: Dordrecht, The Netherlands, 1981; p 331.
(45) Case, D. A.; Darden, T. A.; Cheatham, T. E. I.; Simmerling, C. L.; Wang, J.; Duke, R. E.; Luo, R.; Merz, V.; Pearlman, D. A.; Crowley, V.; Walker, R. C.; Zhang, W.; Wang, B.; Hayik, S.; Roitberg, A.; Seabra, G.; Wong, K. F.; Paesani, F.; Wu, X.; Brozell, S.; Tsui, V.; Gohlke, H.; Yang, L.; Tan, C.; Mongan, J.; Hornak, V.; Cui, G.; Beroza, P.; Mathews, D. H.; Schafmeister, C.; Ross, W. S.; Kollman, P. A. *AMBER 9*, 9th ed.; University of California: San Francisco, CA, 2006.
(46) Singh, U. C.; Kollman, P. A. *J. Comput. Chem.* **1984**, *5*, 129. Besler, B. H.; Merz, K. M. Jr.; Kollman, P. A. *J. Comput. Chem.* **1990**, *11*, 431.
(47) Jorgensen, W. L.; Chandrasekhar, J.; Madura, J. D.; Impey, R. W.; Klein, M. L. *J. Chem. Phys.* **1983**, *79*, 926.
(48) MacKerell, A. D.; Bashford, D.; Bellott, M.; Dunbrack, R. L.; Evanseck, J. D.; Field, M. J.; Fischer, S.; Gao, J.; Guo, H.; Ha, S.; Joseph-McCarthy, D.; Kuchnir, L.; Kuczera, K.; Lau, F. T. K.; Mattos, C.; Michnick, S.; Ngo, T.; Nguyen, D. T.; Prodhom, B.; Reiher, W. E.; Roux, B.; Schlenkrich, M.; Smith, J. C.; Stote, R.; Straub, J.; Watanabe, M.; Wiorkiewicz-Kuczera, J.; Yin, D.; Karplus, M. *J. Phys. Chem. B* **1998**, *102*, 3586.
(49) Mulliken, R. S. *J. Chem. Phys.* **1955**, *23*, 1833.
(50) van der Spoel, D.; Lindahl, E.; Hess, B.; van Buuren, A. R.; Apol, E.; Meulenhoff, P. J.; Tieleman, D. P.; Sijbers, A. L. T. M.; Feenstra, K. A.; van Drunen, R.; Berendsen, H. J. C. *GROMACS User Manual*, version 3.2; University of Groningen: Groningen, The Netherlands, 2002.
(51) Hess, B.; Kutzner, C.; van der Spoel, D.; Lindahl, E. *J. Chem. Theory Comput.* **2008**, *4*, 435. Van der Spoel, D.; Lindahl, E.; Hess, B.; Groenhof, G.; Mark, A. E.; Berendsen, H. J. C. *J. Comput. Chem.* **2005**, *26*, 1701.
(52) Lindahl, E.; Hess, B.; van der Spoel, D. *J. Mol. Model.* **2001**, *7*, 306.
(53) Parrinello, M.; Rahman, A. *J. Appl. Phys.* **1981**, *52*, 7182.
(54) Nosé, S. *Mol. Phys.* **1984**, *52*, 525.
(55) Essman, U.; Perela, L.; Berkowitz, M. L.; Darden, T.; Lee, H.; Pedersen, L. G. *J. Chem. Phys.* **1995**, *103*, 8577.
(56) Miyamoto, S.; Kollman, P. A. *J. Comput. Chem.* **1992**, *13*, 952.
(57) Hess, B. *J. Chem. Theory Comput.* **2008**, *4*, 116.
(58) Biocomputing: Peter Teileman. http://moose.bio.ucalgary.ca/index.php?page=Peter_Tieleman (accessed April 05, 2011). Tieleman, D. P.; Berendsen, H. J. C. *Biophys. J.* **1998**, *74*, 2786.
(59) Morozova, Y. P.; Zharkova, O. M.; Balakina, T. Y.; Artyukohov, V. Y. *J. Appl. Spectrosc.* **2009**, *76*, 312.
(60) Huang, Y.; Li, X. Y.; Fu, K. X.; Zhu, Q. *J. Theor. Comput. Chem.* **2006**, *5*, 355.
(61) Samanta, A.; Fessenden, R. W. *J. Phys. Chem. A* **2000**, *104*, 8972.
(62) Scalmani, G.; Frisch, M. J.; Mennucci, B.; Tomasi, J.; Cammi, R.; Barone, V. *J. Chem. Phys.* **2006**, *124*, 094107.
(63) Cancès, E.; Mennucci, B.; Tomasi, J. *J. Chem. Phys.* **1997**, *107*, 3032. Mennucci, B.; Cancès, E.; Tomasi, J. *J. Phys. Chem. B* **1997**, *101*, 10506.
(64) Marsh, D. *CRC Handbook of Lipid Bilayers*; CRC Press: Boca Raton, FL, 1990.
(65) Janiak, M. J.; Small, D. M.; Shipley, G. G. *J. Biol. Chem.* **1979**, *254*, 6068. Lis, L. J.; McAlister, M.; Fuller, N.; Rand, R. P.; Parsegain, V. A. *Biophys. J.* **1982**, *37*, 657. Lewis, B. A.; Engelman, D. M. *J. Mol. Biol.* **1983**, *166*, 211. De Young, L. R.; Dill, K. A. *Biochemistry* **1988**, *27*, 5281. Rand, R. P.; Parsegain, V. A. *Biochim. Biophys. Acta* **1989**, *988*, 351. Petrache, H. I.; Dodd, S. W.; Brown, M. F. *Biophys. J.* **2000**, *79*, 3172. Balbayý, P.; Dubničková, M.; Kučerka, N.; Kiselev, M. A.; Yaradaikin, S. P.; Uhrková, D. *Biochim. Biophys. Acta* **2001**, *1512*, 40.
(66) Kučerka, N.; Liu, Y.; Chu, N.; Petrache, H. I.; Tristram-Nagle, S.; Nagle, J. F. *Biophys. J.* **2005**, *88*, 2626.
(67) Chiu, S. W.; Pandit, S. A.; Scott, H. L.; Jakobsson, E. *J. Phys. Chem. B* **2009**, *113*, 2748.
(68) Berendsen, H. J. C.; Grigera, J. R.; Straatsma, T. P. *J. Phys. Chem.* **1987**, *91*, 6269.
(69) de Joannis, J.; Jiang, Y.; Yin, F.; Kindt, J. T. *J. Phys. Chem. B.* **2006**, *110*, 25875.
(70) Poger, D.; Van Gunsteren, W. F.; Mark, A. E. *J. Comput. Chem.* **2009**, *31*, 1117.
(71) Poger, D.; Mark, A. E. *J. Chem. Theory Comput.* **2010**, *6*, 325.
(72) Cheng, J. X.; Pautot, S.; Weitz, D. A.; Xie, X. S. *Proc. Natl. Acad. Sci. U.S.A.* **2003**, *100*, 9826. Higgins, M. J.; Polcik, M.; Fukuma, T.; Sader, J. E.; Nakayama, Y.; Jarvis, S. P. *Biophys. J.* **2006**, *91*, 2532. Fukuma, T.; Higgins, M. J.; Jarvis, S. P. *Biophys. J.* **2007**, *92*, 3603.